Inorganic Chemistry
Article
Cite This: Inorg. Chem. XXXX, XXX, XXX−XXX
pubs.acs.org/IC

Unprecedented Formation of a Binuclear Au(II)−Au(II) Complex through Redox State Cycling: Electrochemical Interconversion of Au(I)−Au(I), Au(II)−Au(II), and Au(I)−Au(III) in Binuclear Complexes Containing the Carbanionic Ligand $C_6F_4PPh_2$

Chencheng Sun,[†,§,∥] Nedaossadat Mirzadeh,[*,‡,∥] Si-Xuan Guo,[†] Jiezhen Li,[†] Zhengkui Li,[§] Alan M. Bond,[*,†] Jie Zhang,[*,†] and Suresh K. Bhargava[*,‡]

[†]School of Chemistry, Monash University, Clayton, Victoria 3800, Australia
[‡]School of Science, RMIT University, GPO Box 2476, Melbourne, Victoria 3001, Australia
[§]School of the Environment, Nanjing University, Nanjing 210046, P. R. China

ABSTRACT: The rational design of binuclear Au(I)−Au(I), Au(II)−Au(II), and Au(I)−Au(III) complexes requires an understanding of how the redox states interconvert. Herein, the electrochemical interconversion of the three oxidation states I, II, and III is reported on the voltammetric (cyclic and rotating disk electrode) time scales for binuclear gold complexes containing $C_6F_4PPh_2$ as a ligand, to demonstrate for the first time formation of a binuclear Au(II)−Au(II) from a Au(I)−Au(III) complex. Results are supported by bulk electrolysis and coulometry with reaction products being identified by ^{31}P NMR and UV−vis spectroscopy. All electrochemical processes involve an overall two-electron charge-transfer process with no one-electron intermediate being detected. Importantly, the kinetically rather than thermodynamically favored isomer $[Au_2^{II}X_2(\mu\text{-}2\text{-}C_6F_4PPh_2)_2]$ is formed on redox cycling of $[XAu^{I}(\mu\text{-}2\text{-}C_6F_4PPh_2)(\kappa^2\text{-}2\text{-}C_6F_4PPh_2)Au^{III}X]$ ($X = Cl$, ONO_2). Finally, a mechanism is proposed to explain the simultaneous change of coordination of the chelating carbanionic ligand to bridging mode and interconversion of oxidation states in binuclear gold complexes.

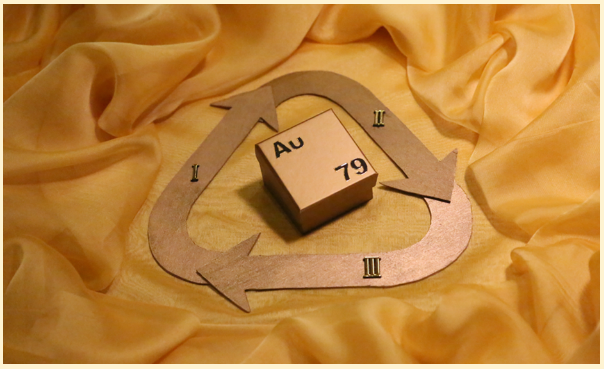

■ INTRODUCTION

In addition to a variety of ligands which have played significant roles in the development of gold chemistry,[1,2] the use of fluorine-substituted carbanions $2\text{-}C_6F_4PPh_2^-$ has enabled the preparation of a diverse range of mono- and binuclear gold complexes in which the formal oxidation state of the metal is I, II, III, or mixed I/III.[3−8] The ligand has established itself recently as a desirable motif for preparation of gold-based therapeutic agents.[8]

Digold(I) complexes of the type $[Au_2(\mu\text{-}2\text{-}C_6F_4PPh_2)_2]$ (**1**, in Scheme 1)[3,4] are prone to oxidation and can readily undergo two-center, two-electron oxidative addition reactions with halogens to form Au(II)−Au(II) complexes $[Au_2X_2(\mu\text{-}2\text{-}C_6F_4PPh_2)_2]$ (X = halide) [X = Cl (**2**), Scheme 1].[4] Compound **2** is thermodynamically unstable and rearranges in solution to form the Au(I)−Au(III) complex $[ClAu(\mu\text{-}2\text{-}C_6F_4PPh_2)(\kappa^2\text{-}2\text{-}C_6F_4PPh_2)AuCl]$ **3** (Scheme 1), in which Au(I) is linearly coordinated by a halide atom and the donor atom of the bridging group and the Au(III) atom is coordinated by a halide atom and the carbanion in a four-membered chelate ring.[4]

Changes in the ligand framework can cause subtle or extreme changes in the chemistry of metal complexes containing carbanion ligands of the type $2\text{-}C_6R_4ER'_2$ (R = hydrogen, halogen, alkyl; E = phosphorus, arsenic; R′ = phenyl, alkyl).[3,9] For example, the 6-methyl substituted complex $[Au_2(\mu\text{-}C_6H_3\text{-}6\text{-}Me\text{-}2\text{-}PPh_2)_2]$ behaves similarly to its tetrafluoro analogue. However, isomerization from Au(II)−Au(II) to Au(I)−Au(III) is much faster in the $6\text{-}MeC_6H_3\text{-}2\text{-}PPh_2$ system than in the $2\text{-}C_6F_4PPh_2$ one; the former occurs below room temperature within minutes, whereas the latter requires hours in hot toluene.[10] These data imply that Au(I)−Au(III) is the thermodynamically favored isomer.

Intriguingly, replacement of fluorine by hydrogen atoms in the carbanion leads to the formation of the C−C coupled Au(I)−Au(I) complex $[Au_2X_2(2,2'\text{-}Ph_2PC_6H_4C_6H_4PPh_2)]$ as the result of reductive elimination reaction at a Au(II)−Au(II) center,[11,12] a completely different reduction pathway to that observed in the $C_6F_4PPh_2$ system.[4]

Received: July 4, 2019

DOI: 10.1021/acs.inorgchem.9b01983
Inorg. Chem. XXXX, XXX, XXX−XXX

Scheme 1. Interconversion of Oxidation States I, II, and III in Binuclear Gold Complexes Containing the $C_6F_4PPh_2^-$ Ligand

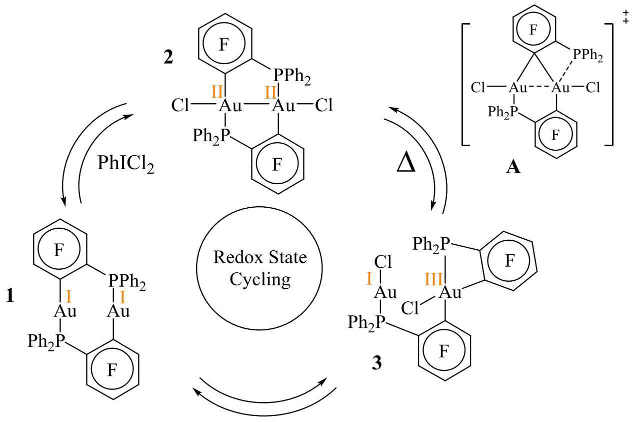

Our interest in exploring the extensive redox behavior of binuclear gold complexes containing 2-$C_6F_4PPh_2$ has now resulted in an electrochemical study which has provided the first observation of interconversion of oxidation states I, II, and III in digold complexes containing the carbanionic ligand $C_6F_4PPh_2$; a detailed account is presented here.

■ RESULTS AND DISCUSSION

Cyclic Voltammetry of Dinuclear Gold Complexes $[Cl_2Au_2^{II}(\mu\text{-}2\text{-}C_6F_4PPh_2)_2]$ (2) and $[(ONO_2)_2Au_2^{II}(\mu\text{-}2\text{-}C_6F_4PPh_2)_2]$ (4): Influence of the Axial Ligand. Cyclic voltammograms at a scan rate of 2 V s^{-1} were obtained with 1.0 mM **2** (Figure 1A) or 1.0 mM **4** (Figure 1B) at a glassy carbon electrode in CH_2Cl_2 (0.1 M Bu_4NPF_6). For **2**, when the potential was initially scanned positively from the open circuit value of −0.30 to 1.35 V vs $Fc^{0/+}$, no oxidation process was observed. However, on reversing the scan direction, a well-defined irreversible reduction process (labeled 1) was detected at −0.89 V. In the second scan, in the positive potential direction, two new oxidation processes (labeled 2 and 3) were detected at 0.91 and 1.20 V and are associated with oxidation of the products of reduction process 1. Oxidation process 3 is coincident with oxidation of Cl^- from Et_4NCl or PPh_4Cl, implying that Cl^- is released upon reduction of **2**. Consequently, process 2 corresponds to the oxidation of digold(I) back to digold(II). Reduction process 1 therefore is attributed to an overall two-electron reduction of $[Cl_2Au_2^{II}(\mu\text{-}2\text{-}C_6F_4PPh_2)_2]$ (**2**) to $[Au_2^{I}(\mu\text{-}2\text{-}C_6F_4PPh_2)_2]$ (**1**) along with elimination of Cl^-, as outlined in eq 1.

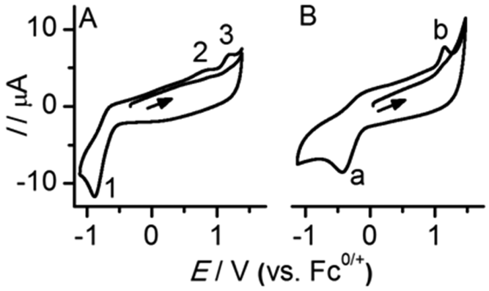

Figure 1. Cyclic voltammograms obtained at a scan rate of 2 V s^{-1} for (A) 1.0 mM $[Cl_2Au_2^{II}(\mu\text{-}2\text{-}C_6F_4PPh_2)_2]$ (**2**) or (B) 1.0 mM $[(ONO_2)_2Au_2^{II}(\mu\text{-}2\text{-}C_6F_4PPh_2)_2]$ (**4**) at a glassy carbon electrode (diameter of 1 mm) in CH_2Cl_2 (0.1 M Bu_4NPF_6).

$$[Cl_2Au_2^{II}(\mu\text{-}2\text{-}C_6F_4PPh_2)_2]\ (\mathbf{2}) + 2e^- \rightarrow [Au_2^{I}(\mu\text{-}2\text{-}C_6F_4PPh_2)_2]\ (\mathbf{1}) + 2Cl^- \qquad (1)$$

The digold(II)−dinitrate complex $[(ONO_2)_2Au_2^{II}(\mu\text{-}2\text{-}C_6F_4PPh_2)_2]$ (**4**) in CH_2Cl_2 displays an analogous irreversible reduction process (labeled a) under conditions of cyclic voltammetry but now at −0.43 V, which is 0.46 V more positive than **2**, reflecting the easier reducibility of the Au(II)−Au(II) center with the axial ligand of ONO_2. However, whether the origin of this difference is thermodynamic or kinetic is unknown. For **4**, only a single new oxidation process (labeled b) is observed in the second positive potential scan at a potential of 1.15 V, which is attributed to the oxidation of digold(I) back to digold(II). Process a is proposed to be the overall two-electron reduction of $[(ONO_2)_2Au_2^{II}(2\text{-}\mu\text{-}C_6F_4PPh_2)_2]$ (**4**) to $[Au_2^{I}(2\text{-}\mu\text{-}C_6F_4PPh_2)_2]$ (**1**) with elimination of NO_3^-, as outlined in eq 2, with process b being the oxidation of the digold(I) species to reform **4**.

$$[(ONO_2)_2Au_2^{II}(2\text{-}\mu\text{-}C_6F_4PPh_2)_2]\ (\mathbf{4}) + 2e^- \rightarrow [Au_2^{I}(2\text{-}\mu\text{-}C_6F_4PPh_2)_2]\ (\mathbf{1}) + 2NO_3^- \qquad (2)$$

Electrochemical oxidation of either **2** or **4** was not observed within the anodic limit of the solvent potential window. This is not surprising since oxidation of Au(I)−Au(I) to Au(II)−Au(II) already requires very positive potentials as shown in the second cycle of Figure 1.

Cyclic Voltammetry of $[ClAu^{I}(\mu\text{-}2\text{-}C_6F_4PPh_2)(\kappa^2\text{-}2\text{-}C_6F_4PPh_2)Au^{III}Cl]$ (3) and $[(O_2NO)Au^{I}(\mu\text{-}2\text{-}C_6F_4PPh_2)(\kappa^2\text{-}2\text{-}C_6F_4PPh_2)Au^{III}(ONO_2)]$ (5). The cyclic voltammograms obtained at a scan rate of 2 V s^{-1} with 1.0 mM **3** (Figure 2A) or 1.0 mM **5** (Figure 2B) at a glassy carbon electrode in CH_2Cl_2 (0.1 M Bu_4NPF_6) differ significantly from **2** and **4**. **3** exhibited an irreversible reduction process (labeled 4′) at −1.68 V, which is 0.79 V more negative than that for $[Cl_2Au_2^{II}(2\text{-}\mu\text{-}C_6F_4PPh_2)_2]$ (**2**), reflecting the greater difficulty of reducing the Au(III)−carbon δ-bond. However, in the reverse positive direction scan, the two oxidation processes (labeled 2′ and 3′) occur at very similar potentials to those for 2 and 3 in Figure 1A, implying that reduction process 4′ generates the same products as reduction process 1. However, following the oxidation processes 2′ and 3′, in the second

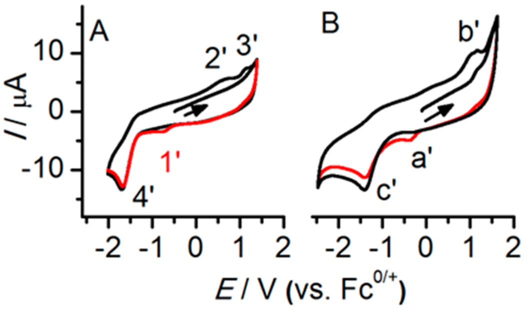

Figure 2. Cyclic voltammograms obtained at a scan rate of 2 V s^{-1} with a glassy carbon electrode (diameter of 1 mm) in CH_2Cl_2 (0.1 M Bu_4NPF_6) for (A) 1.0 mM $[ClAu^{I}(\mu\text{-}2\text{-}C_6F_4PPh_2)(\kappa^2\text{-}2\text{-}C_6F_4PPh_2)Au^{III}Cl]$ (**3**) and (B) 1.0 mM $[(O_2NO)Au^{I}(\mu\text{-}2\text{-}C_6F_4PPh_2)(\kappa^2\text{-}2\text{-}C_6F_4PPh_2)Au^{III}(ONO_2)]$ (**5**).

negative potential direction scan, a second reduction process (labeled 1′) emerged at a potential of −0.82 V which is consistent with reduction of $[\mathrm{Cl_2Au_2^{II}(2\text{-}C_6F_4PPh_2)_2}]$ (**2**).

When the potential was switched before oxidation process 3′, reduction process 1′ remained. However, if the potential was switched prior to oxidation process 2′, reduction process 1′ was absent. The results imply that reduction process 1′ is derived from the product of oxidation process 2′. Thus, oxidation processes 2 and 2′ are both due to the oxidation of $[\mathrm{Au_2^{I}(2\text{-}C_6F_4PPh_2)_2}]$ (**1**) to $[\mathrm{Au_2^{II}Cl_2(2\text{-}C_6F_4PPh_2)_2}]$ (**2**), so that on redox cycling, the kinetically stable isomer **2** is favored over the thermodynamically favored one, as in eqs 3 and 4.

$$[\mathrm{ClAu^{I}(\mu\text{-}2\text{-}C_6F_4PPh_2)(\kappa^2\text{-}2\text{-}C_6F_4PPh_2)Au^{III}Cl}]\ (\mathbf{3}) + 2e^- \rightarrow [\mathrm{Au_2^{I}(\mu\text{-}2\text{-}C_6F_4PPh_2)_2}]\ (\mathbf{1}) + 2\mathrm{Cl}^- \tag{3}$$

$$[\mathrm{Au_2^{I}(\mu\text{-}2\text{-}C_6F_4PPh_2)_2}]\ (\mathbf{1}) + 2\mathrm{Cl}^- \rightarrow [\mathrm{Cl_2Au_2^{II}(\mu\text{-}2\text{-}C_6F_4PPh_2)_2}]\ (\mathbf{2}) + 2e^- \tag{4}$$

$[\mathrm{(O_2NO)Au^{I}(\mu\text{-}2\text{-}C_6F_4PPh_2)(\kappa^2\text{-}2\text{-}C_6F_4PPh_2)Au^{III}(ONO_2)}]$ (**5**) in $\mathrm{CH_2Cl_2}$ displays (Figure 2B) an irreversible reduction process (labeled c′) at −1.41 V, which is 0.98 V more negative (Figure 1B) than for digold(II)-$(\mathrm{ONO_2})_2$, establishing the greater difficulty in reducing the Au(III)−carbon *δ*-bond. However, this peak potential is 0.27 V less negative than the reduction peak for digold(I,III)-$\mathrm{Cl_2}$, reflecting the easier reducibility when the axial ligand is $-\mathrm{ONO_2}$. For **5**, on the second scan in the positive potential direction, an oxidation process (labeled b′) is observed at a similar potential to that for process b in Figure 1B. Additionally, after oxidation process b′ and reversing the scan direction, a new reduction process (labeled a′) emerges at a potential −0.42 V, consistent with reduction of $[\mathrm{(ONO_2)_2Au_2^{II}(\mu\text{-}2\text{-}C_6F_4PPh_2)_2}]$ (**4**). When the potential was switched prior to oxidation process b′, reduction process a′ was absent confirming that reduction process a′ is associated with the product of oxidation process b′. This again confirms that the oxidation processes b and b′ are both due to the oxidation of $[\mathrm{Au_2^{I}(2\text{-}\mu\text{-}C_6F_4PPh_2)_2}]$ (**1**). Again, on redox cycling, the thermodynamically favored Au(I)−Au(III) isomer is converted to the kinetically favored isomer, as in eqs 5 and 6.

$$[\mathrm{(O_2NO)Au^{I}(\mu\text{-}2\text{-}C_6F_4PPh_2)(\kappa^2\text{-}2\text{-}C_6F_4PPh_2)Au^{III}(ONO_2)}]\ (\mathbf{5}) + 2e^- \rightarrow [\mathrm{Au_2^{I}(2\text{-}\mu\text{-}C_6F_4PPh_2)_2}]\ (\mathbf{1}) + 2\mathrm{NO_3}^- \tag{5}$$

$$[\mathrm{Au_2^{I}(\mu\text{-}2\text{-}C_6F_4PPh_2)_2}]\ (\mathbf{1}) + 2\mathrm{NO_3}^- \rightarrow [\mathrm{(ONO_2)_2Au_2^{II}(\mu\text{-}2\text{-}C_6F_4PPh_2)_2}]\ (\mathbf{4}) + 2e^- \tag{6}$$

Determination of the Diffusion Coefficients and Number of Electrons Transferred. In order to quantitatively determine the diffusion coefficients and the number of electrons transferred in the reduction of the four dinuclear gold compounds, steady-state voltammetric data were obtained and analyzed in combination with the chronoamperometric (coulometric) data derived from bulk electrolysis. The steady-state limiting current, I_{ss}, obtained at a rotating disk electrode is given by the Levich equation[13] (eq 7)

$$I_{ss} = 0.62nFAD^{2/3}\omega^{1/2}\nu^{-1/6}c^* \tag{7}$$

where n is the total number of electrons transferred; F is Faraday's constant (96485 C $\mathrm{mol^{-1}}$); A is the area of the working electrode (0.0707 $\mathrm{cm^2}$); D and c^* are the diffusion coefficient and concentration of the gold compound, respectively; ω ($=2\pi f$) is the angular frequency of rotation; and ν is the kinematic viscosity of $\mathrm{CH_2Cl_2}$ (at 20 °C, ν = viscosity/density = 0.43/1.3266 $\mathrm{cm^2\ s^{-1}}$ = 0.32 $\mathrm{cm^2\ s^{-1}}$).

RDE voltammograms for compounds **2** and **4** are shown in Figure 3 as a function of rotation rate. The D values obtained from the Levich equation using n = 2.0 were (1.2 ± 0.1) × 10^{-5} (**2**) and (1.3 ± 0.1) × 10^{-5} $\mathrm{cm^2\ s^{-1}}$ (**3**, **4**, **5**).

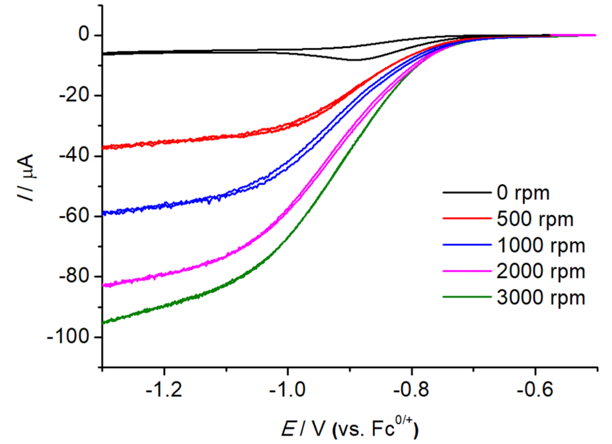

Figure 3. RDE voltammograms obtained as a function of rotation rate for reduction of 1.0 mM $[\mathrm{Cl_2Au_2^{II}(\mu\text{-}2\text{-}C_6F_4PPh_2)_2}]$ (**2**) in $\mathrm{CH_2Cl_2}$ (0.1 M $\mathrm{Bu_4NPF_6}$) with a 3 mm diameter GC rotating disk electrode. Scan rate = 20 mV $\mathrm{s^{-1}}$.

Coulometric analysis of the current−time derived from controlled potential bulk electrolysis of the gold compounds gives the charge (Q, coulomb) calculated by eq 8,[11] where V is the volume of the solution (10 mL). n values of 1.8 ± 0.2 (**2**), 1.9 ± 0.2 (**3**), 1.9 ± 0.2 (**4**), and 2.1 ± 0.2 (**5**) were obtained via coulometric analysis.

$$Q = nFVc^* \tag{8}$$

It is likely that the overall electroreduction of digold(II)−dichloride proceeds by a one-electron reduced intermediate. However, cyclic voltammetry of digold(II)−dichloride with a 50 *μ*m diameter Pt microelectrode at scan rates up to 100 V $\mathrm{s^{-1}}$ and lower temperature (−15 °C) did not allow detection of intermediates, probably due to their very high level of reactivity.

Characterization of Products after Bulk Electrolysis by RDE Voltammetry, UV−Vis, and ^{31}P NMR Spectroscopies. In order to unequivocally identify the product(s) derived from the irreversible reduction of **2**, **3**, **4**, or **5**, bulk electrolysis experiments were undertaken with 1.0 mM of gold compound using a glassy carbon tube working electrode. RDE voltammetry along with UV−vis and ^{31}P NMR spectroscopy on solutions obtained after bulk electrolysis were used to identify the products.

Bulk electrolysis of $[\mathrm{Cl_2Au_2^{II}(\mu\text{-}2\text{-}C_6F_4PPh_2)_2}]$ (**2**) in $\mathrm{CH_2Cl_2}$ with an applied potential of −0.9 V (vs $\mathrm{Fc^{0/+}}$) led to a color change from yellow to colorless. As shown in Figure 4A, RDE voltammetry before and after the reductive bulk electrolysis of **2** leads to transition from a fully reductive to a fully oxidative process. Bulk electrolysis of digold(I,III)−dichloride (**3**) with an applied potential of −1.8 V (vs $\mathrm{Fc^0/^+}$) also exhibits an almost complete transition from a reductive to

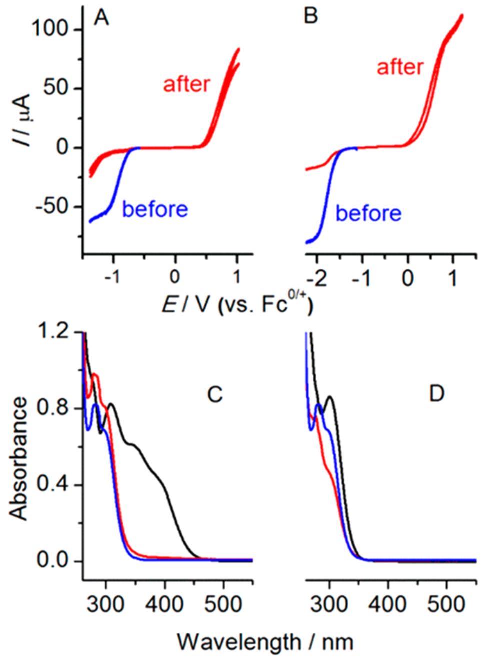

Figure 4. RDE voltammograms obtained before and after reductive bulk electrolysis of (A) 1.0 mM $[Cl_2Au_2^{II}(\mu\text{-}2\text{-}C_6F_4PPh_2)_2]$ (**2**) and (B) 1.0 mM $[ClAu^I(\mu\text{-}2\text{-}C_6F_4PPh_2)(\kappa^2\text{-}2\text{-}C_6F_4PPh_2)Au^{III}Cl]$ (**3**) in CH_2Cl_2 (0.05 M Bu_4NPF_6) using a scan rate of 20 mV s^{-1} and rotation rate of 1000 rpm. UV−visible spectra of (C) 0.05 mM $[Cl_2Au_2^{II}(\mu\text{-}2\text{-}C_6F_4PPh_2)_2]$ (**2**) and (D) 0.05 mM $[ClAu^I(\mu\text{-}2\text{-}C_6F_4PPh_2)(\kappa^2\text{-}2\text{-}C_6F_4PPh_2)Au^{III}Cl]$ (**3**) before (black line) and after (red line) exhaustive electrolysis. The spectrum of 0.05 mM digold(I) (blue line) is also shown for comparison. For the electrolysis of $[Cl_2Au_2^{II}(\mu\text{-}2\text{-}C_6F_4PPh_2)_2]$ (**2**), the potential was held at −0.9 V, while for $[ClAu^I(\mu\text{-}2\text{-}C_6F_4PPh_2)(\kappa^2\text{-}2\text{-}C_6F_4PPh_2)Au^{III}Cl]$ (**3**), the potential was held at −1.8 V vs Fc$^{0/+}$.

an oxidative process (Figure 4B) when monitored by RDE voltammetry. Figures 4C and D show the UV−visible spectra of $[Cl_2Au_2^{II}(\mu\text{-}2\text{-}C_6F_4PPh_2)_2]$ (**2**) and $[ClAu^I(\mu\text{-}2\text{-}C_6F_4PPh_2)(\kappa^2\text{-}2\text{-}C_6F_4PPh_2)Au^{III}Cl]$ (**3**), respectively, before and after bulk electrolysis of 1.0 mM solutions followed by a 20-fold dilution. The spectrum of 0.05 mM $[Au_2^I(\mu\text{-}2\text{-}C_6F_4PPh_2)_2]$ (**1**) is also shown for comparison.

The ^{31}P NMR spectrum after bulk electrolysis of digold(II)−dichloride (**2**) contains a resonance at δ 41.4, together with the expected septet from the supporting electrolyte anion $[PF_6]^-$. The resonance at δ 41.5 closely matches the ^{31}P NMR spectrum of digold(I). Bulk electrolysis of digold(II)−dinitrate **4** in CH_2Cl_2 with an applied potential of −0.5 V (vs Fc$^{0/+}$) also led to a color change from yellow to colorless. The ^{31}P NMR spectrum after bulk electrolysis contained a resonance at δ 41.4, which again corresponds to formation of the digold(I) compound (**1**). NMR spectroscopy identification of the products therefore confirms that the reduction of $[Cl_2Au_2^{II}(\mu\text{-}2\text{-}C_6F_4PPh_2)_2]$ (**2**) and $[(ONO_2)_2Au_2^{II}(\mu\text{-}2\text{-}C_6F_4PPh_2)_2]$ (**4**) occur be an overall two-electron reductive elimination reactions to give $[Au_2^I(\mu\text{-}2\text{-}C_6F_4PPh_2)_2]$ (**1**) with cleavage of the Au(II)−Au(II) bond and the Au(II)−Cl or Au(II)−ONO_2 bond, respectively.

The ^{31}P NMR spectrum after bulk electrolysis of digold(I,III)−dichloride (**3**) contains a singlet at δ 41.4 (corresponding to the digold(I) compound) and a triplet at δ −9.0, −14.9, and −20.8, due to $PO_2F_2^-$, a hydrolysis product of PF_6^-. Reduction at very negative potentials under bulk electrolysis condition can lead to PF_6^- hydrolysis. It is now spectroscopically confirmed that reduction of $[ClAu^I(\mu\text{-}2\text{-}C_6F_4PPh_2)(\kappa^2\text{-}2\text{-}C_6F_4PPh_2)Au^{III}Cl]$ (**3**) in CH_2Cl_2 results in the cleavage of the Au(III)−carbon δ-bond and the generation of $[Au_2^I(2\text{-}C_6F_4PPh_2)_2]$ (**1**), as shown in eq 3.

Bulk electrolysis of digold(I,III)−dinitrate (**5**) at −1.5 V (vs Fc$^{0/+}$) in CH_2Cl_2 (0.1 M Bu_4NPF_6) gave a ^{31}P NMR spectrum which also contains a singlet at δ 41.4, along with a resonance at δ 44.8, assigned to tetragold(I) $[Au_4^I(\mu\text{-}2\text{-}C_6F_4PPh_2)_4]$ (**6**) (Figure 5),[4] also obtained a very small amount of $PO_2F_2^-$, a hydrolysis product of PF_6^- (see above). Thus, during the exhaustive reduction of $[(O_2NO)Au^I(\mu\text{-}2\text{-}C_6F_4PPh_2)(\kappa^2\text{-}2\text{-}C_6F_4PPh_2)Au^{III}(ONO_2)]$ (**5**), cleavage of the Au(III)−carbon δ-bond to generate $[Au_2^I(\mu\text{-}2\text{-}C_6F_4PPh_2)_2]$ (**1**) occurs along with the formation of $[Au_4^I(\mu\text{-}2\text{-}C_6F_4PPh_2)_4]$ (**6**), the ^{31}P NMR of which appears at 44.8, ca. 4 ppm higher frequency from that for **1**.[4] Compounds **1** and **6** are formed in a 2:1 ratio under electrochemical reduction conditions; repeated chemical preparations of **6** give mixtures of **1** and **6** in varying proportions.[4]

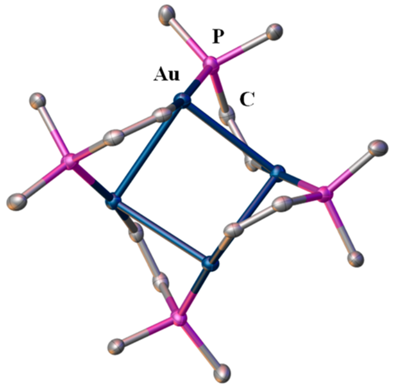

Figure 5. Molecular structure of tetragold(I) $[Au_4^I(\mu\text{-}2\text{-}C_6F_4PPh_2)_4]$ (**6**). Ellipsoids show 30% probability levels, and hydrogen atoms have been omitted for clarity. Only the *ipso* carbons of the phenyl groups attached to the phosphorus atoms are shown. Only the two carbon atoms of the C_6F_4 ring that form the macrocycle are shown.

From these results it appears that the rearrangement of Au(I)−Au(III) to Au(II)−Au(II) proceeds via σ-aryl migration. One-ended dissociation of the chelating group allows the carbanion to transfer from one gold atom and reassociate with the neighboring gold atom via a two-electron, three-center transition (stage A, shown in Scheme 1). This transition state is supported by an ab initio calculation of the isomerization of Au(II)−Au(II) complexes $[Au_2X_2(\mu\text{-}2\text{-carbanion})_2]$ (X = Cl, Br, I; carbanion = $C_6H_4PPh_2$, C_6H_3-*n*-Me-2-PPh_2 *n* = 5, 6).[14] A related mechanism is assumed to apply when **3** (or **5**) is reduced to **2** (or **4**) and **1**.

Comparison with the Chemical Reduction of the Dinuclear Gold Complexes. Based on the electrochemical observations, digold(II)−dichloride (**2**) is much easier to reduce than digold(I,III)−dichloride (**3**). Consistent with these observations, **2** but not **3** is reduced to the parent digold(I) **1** (^{31}P NMR evidence) by zinc powder, which is a moderately strong reductant. In contrast, digold(I,III)−dinitrate (**5**) undergoes rapid and clean reduction to **1**, in the presence of sodium ethanethiolate. No intermediates were identified during the course of reaction by ^{31}P NMR spectroscopy. Interestingly, compound **3** is reduced to **1** in the presence of sodium ethanethiolate, although it is noted that this reaction involves the formation and subsequent reaction of intermediate species evident from ^{31}P NMR spectra.

CONCLUSION

In conclusion, we have presented the first electrochemical investigation of interconversion of various oxidation states (I, II, and III) in binuclear gold complexes containing the 2-Br-$C_6F_4PPh_2$ ligand. This ligand is well-established in organogold chemistry and displays two coordination modes, chelate and bridging; the interconversion of the former to the latter has not been reported until now.[3,5] We also report the electrochemical formation of the kinetically rather than thermodynamically favored isomer gold(II)−gold(II) $[Au_2^{II}X_2(\mu\text{-}2\text{-}C_6F_4PPh_2)_2]$ from the redox cycling of gold(I)−gold(III) $[XAu^I(\mu\text{-}2\text{-}C_6F_4PPh_2)(\kappa^2\text{-}2\text{-}C_6F_4PPh_2)Au^{III}X]$ (X = Cl, NO_3). A mechanism to describe this rare behavior has been proposed.

An understanding of how gold I, II, and III oxidation states interconvert provides a pathway for the rational design of gold complexes. This report aims at realizing the potential of manipulation of oxidation states in gold complexes, a critical factor in fine-tuning their chemical properties.

EXPERIMENTAL SECTION

Chemicals and Reagents. Dichloromethane (CH_2Cl_2, Aldrich) is of HPLC grade, and acetone (BDH) is of laboratory reagent grade. Ferrocene (BDH), tetraethylammonium chloride (Et_4NCl), tetraphenylphosphonium chloride (PPh_4Cl), zinc powder, and sodium ethanethiolate (Sigma-Aldrich) were used as received. Tetrabutylammonium hexafluorophosphate (Bu_4NPF_6) (GFS) was purified according to literature procedures[15] and used as the supporting electrolyte in dichloromethane.

Instrumentation. ^{31}P NMR spectra, referenced to external 85% H_3PO_4 (^{31}P), were recorded on a Bruker DPX 400 spectrometer at a frequency of 121 MHz. UV−visible spectra over the wavelength range of 250 to 800 nm were obtained with a Cary 5 spectrophotometer (Varian OS/2 software) using a 1 mm path length quartz cuvette.

Preparation of Dinuclear Gold Complexes. The digold complexes **1**−**5** were prepared following established literature procedures.[4]

Electrochemical Instrumentation and Procedures. Voltammetric measurements were conducted in nitrogen degassed CH_2Cl_2 using a CHI 760E electrochemical workstation (CH Instruments, Austin, TX). A silver wire immersed in a glass tube containing 0.1 M Bu_4NPF_6 in CH_2Cl_2 with a frit was used as a quasi-reference electrode. For cyclic voltammetric studies, a glassy carbon disk electrode with a diameter of 1 mm was used as the working electrode, and a platinum wire was used as the auxiliary electrode. For rotating disk electrode (RDE) studies, an ALS rotating disk electrode rotator (RRDE-3A) was connected to the electrochemical workstation. In this case, a 3 mm diameter GC disk was used as the working electrode, along with the same platinum wire auxiliary and reference electrodes used for cyclic voltammetry. Bulk electrolysis was performed inside a nitrogen filled glovebox (oxygen- and moisture-free system). The glassy carbon tube working electrode and the reference electrode were separated from the platinum gauze auxiliary electrode by a fine porosity frit. Ten mL of 1.0 mM of dinuclear gold complex dissolved in CH_2Cl_2 (0.05 M Bu_4NPF_6) was placed in the inner compartment which contained the working and reference electrodes, while 15 mL of CH_2Cl_2 with 0.05 M Bu_4NPF_6 was placed in the outer compartment which contained the platinum gauze auxiliary electrode. During the course of bulk electrolysis, the solutions in both compartments were magnetically stirred. Prior to use, the GC electrodes were polished using an aqueous 0.3 μm Al_2O_3 slurry (Buehler), rinsed thoroughly with distilled water, sonicated, rinsed with water again, finally rinsed with acetone, and dried under nitrogen. All electrochemical studies were undertaken at 20 ± 1 °C. The reference potentials were calibrated to that of the ferrocene/ferricenium ($Fc^{0/+}$) couple.

AUTHOR INFORMATION

Corresponding Authors

*E-mail: nedaossadat.mirzadeh@rmit.edu.au.
*E-mail: alan.bond@monash.edu.
*E-mail: jie.zhang@monash.edu.
*E-mail: suresh.bhargava@rmit.edu.au.

ORCID

Nedaossadat Mirzadeh: 0000-0002-3092-2634
Alan M. Bond: 0000-0002-1113-5205
Jie Zhang: 0000-0003-2493-5209
Suresh K. Bhargava: 0000-0002-3127-8166

Author Contributions

The manuscript was written through contributions of all authors.

Author Contributions

[‖]C.S. and N.M. contributed equally.

Notes

The authors declare no competing financial interest.

ACKNOWLEDGMENTS

Authors acknowledge Dr. Nedaossadat Mirzadeh for use of her artwork 'wheel of gold conversion' as graphical abstract.

REFERENCES

(1) Schmidbauer, H. *Gold: chemistry, biochemistry and technology*, 1st ed.; Wiley: England, 1999.

(2) *Gold chemistry: applications and future directions in the life sciences*; Mohr, F., Ed.; Wiley: Germany, 2009.

(3) Mirzadeh, N.; Bennett, M. A.; Bhargava, S. K. Cycloaurated complexes of aryl carbanions: digold(I), digold(II) and beyond. *Coord. Chem. Rev.* **2013**, *257*, 2250−2273.

(4) Bennett, M. A.; Bhargava, S. K.; Mirzadeh, N.; Privér, S. H.; Wagler, J.; Willis, A. C. Synthesis and interconversions of digold(I), tetragold(I), digold(II), gold(I)-gold(III) and digold(III) complexes of fluorine-substituted aryl carbanions. *Dalton Trans* **2009**, 7537−7551.

(5) Bennett, M. A.; Bhargava, S. K.; Mirzadeh, N.; Privér, S. H. The use of $[2\text{-}C_6R_4PPh_2]^-$(R = H, F) and related carbanions as building blocks in coordination chemistry. *Coord. Chem. Rev.* **2018**, *370*, 69−128.

(6) Bennett, M. A.; Bhargava, S. K.; Takahashi, M.; Mirzadeh, N.; Privér, S. H. ^{197}Au Mössbauer Spectroscopic Studies of Cyclometalated Gold Dimers Containing 2-$C_6F_4PPh_2$ Ligands. *Bull. Chem. Soc. Jpn.* **2009**, *82* (12), 1506−1509.

(7) Bhargava, S. K.; Bennett, M. A.; Mirzadeh, N.; Privér, S. H.; Wagler, J. Trinuclear Mixed-valent Gold Complexes Derived from 2-$C_6F_4PPh_2$: Phosphine Oxide Complexes of Gold(III) and an Ortho-Metallated Complex of Gold(I). *Z. Naturforsch., B: J. Chem. Sci.* **2009**, *64b*, 1463−1468.

(8) Reddy, T. S.; Privér, S. H.; Mirzadeh, N.; Bhargava, S. K. Synthesis of gold(I) phosphine complexes containing the 2-$BrC_6F_4PPh_2$ ligand: Evaluation of anticancer activity in 2D and 3D spheroidal models of HeLa cancer cells. *Eur. J. Med. Chem.* **2018**, *145*, 291−301.

(9) Mohr, F.; Privér, S. H.; Bhargava, S. K.; Bennett, M. A. *Ortho*-metallated transition metal complexes derived from tertiary phosphine and arsine ligands. *Coord. Chem. Rev.* **2006**, *250*, 1851−1888.

(10) Bhargava, S. K.; Mohr, F.; Bennett, M. A.; Welling, L. L.; Willis, A. C. Ortho-metallated transition metal complexes derived from tertiary phosphine and arsine ligands. *Organometallics* **2000**, *19*, 5628−5635.

(11) Bennett, M. A.; Bhargava, S. K.; Griffiths, K. D.; Robertson, G. B. Coupling of cyclometalatedphenylphosphanes in dinuclear gold(II) complexes. *Angew. Chem., Int. Ed. Engl.* **1987**, *26*, 260−261.

(12) Bennett, M. A.; Bhargava, S. K.; Hockless, D. S. R.; Welling, L. L.; Willis, A. C. Dinuclearcycloauratedcomplexes containing bridging (2-diphenylphosphino)phenylphosphine and (2-diethylphosphino)-phenylphosphine, C6H4PR2 (R = Ph, Et). carbon-carbon bond formation by reductive elimination at a gold(II)-gold(II) center. *J. Am. Chem. Soc.* **1996**, *118*, 10469−10478.

(13) Bard, A. J.; Faulkner, L. R. *Electrochemical Methods: Fundamentals and Applications*, 2nd ed.; John Wiley & Sons, Inc.: New York, 2001.

(14) Hermann, H. L.; Schwerdtfeger, P.; Mohr, F.; Bhargava, S. K. Unusual strong ortho effects in the rearrangement of binuclear gold(I) complexes. *Organometallics* **2003**, *22*, 2373−2377.

(15) Kissinger, P. T.; Heineman, W. R. *Laboratory techniques in electroanalytical chemistry*; Marcel Dekker: New York, 1984; DOI: 10.1201/9781315274263.